Caspase Activation and Amyloid Precursor Protein Cleavage in Rat Ocular Hypertension

Stuart J. McKinnon,[1] Donna M. Lehman,[1] Lisa A. Kerrigan-Baumrind,[2] Carol A. Merges,[2] Mary Ellen Pease,[2] Danielle F. Kerrigan,[2] Nancy L. Ransom,[1] N. Grace Tahzib,[1] Herbert A. Reitsamer,[1,3] Hana Levkovitch-Verbin,[2] Harry A. Quigley,[2,4] and Donald J. Zack[2,5]

PURPOSE. Retinal ganglion cell (RGC) death in glaucoma involves apoptosis. Activation of caspases and abnormal processing of amyloid precursor protein (APP) are important events in other chronic neurodegenerations, such as Alzheimer's disease (AD). The retinal expression and activation of caspases and the patterns of caspase-3–mediated APP processing in ocular hypertensive models of rat glaucoma were investigated.

METHODS. RGC death was produced in one eye by chronic exposure to increased intraocular pressure (IOP) or by optic nerve transection. Elevated IOP was produced by obstruction of aqueous humor outflow with laser coagulation or limbal hypertonic saline injection. Caspase activity and APP processing in the retina were examined by RNase protection assay (RPA), immunocytochemistry, immunoblot assay, and colorimetric assay.

RESULTS. RPA revealed elevations of caspase-3 mRNA, as well as other apoptosis-related mRNAs. Immunocytochemistry showed caspase-3 activation in RGCs damaged by ocular hypertension. The generation of the caspase-3–mediated APP cleavage product (ΔC-APP) was also increased in ocular hypertensive RGCs. Western immunoblot assay and colorimetry revealed significantly more activated caspase-3 in ocular hypertensive retinas than in control retinas. The activated form of caspase-8, an initiator caspase, and amyloid-β, a product of APP proteolysis and a component of senile plaques in AD, were detected in RGCs by immunohistochemistry significantly more often in ocular hypertensive than in control retinas. The amounts of full-length APP were reduced and amyloid-β–containing fragments were increased in ocular hypertensive retinas by Western immunoblot assay.

CONCLUSIONS. Rat RGCs subjected to chronic ocular hypertension demonstrate caspase activation and abnormal processing of APP, which may contribute to the pathophysiology of glaucoma. (*Invest Ophthalmol Vis Sci.* 2002;43:1077–1087)

Glaucoma, one of the leading causes of vision loss in the world,[1–3] is an optic neuropathy characterized by retinal ganglion cell (RGC) death, axon loss, and an excavated appearance of the optic nerve head.[4] RGC death mechanisms in experimental animal models of glaucoma and human glaucoma have been shown to involve apoptosis.[5–8] Specific initiators of apoptosis in glaucoma may include blockage of axonal transport leading to neurotrophin depletion,[9–12] glutamate excitotoxicity,[13] antibodies to heat-shock proteins,[14] ischemia,[15] and nitric oxide synthase upregulation with reactive oxygen species formation.[16]

The apoptotic cascade invokes a series of cellular events, many of which have been conserved throughout evolution. Central to the implementation of apoptosis is a class of aspartate-specific proteases of the interleukin-1β–converting enzyme (ICE) family known as caspases. Caspases are translated as inactive precursors having large (20 kDa) and small (10 kDa) domains. Caspase activation involves proteolytic cleavage between the domains, causing association of large and small subunits to form an activated heterodimer. Activated caspases kill cells by degrading structural elements and DNA repair enzymes[17] and by indirect activation of chromosomal endonucleases.[18]

Because of its central role in neuronal death, caspase activation has been the focus of intensive research in chronic neurodegenerations such as Huntington's,[19,20] Parkinson's,[21] and Alzheimer's[22,23] disease. Abnormal processing of amyloid precursor protein (APP), which includes production of amyloid-β (a component of senile plaques), plays an important role in the pathogenesis of Alzheimer's disease (AD). Caspase-3 cleavage sites have been recognized in the APP sequence. Caspase-3 cleavage of the C-terminal cytoplasmic tail of APP yields neurotoxic peptide fragments that upregulate amyloid-β production in dying hippocampal neurons.[24,25] Caspase-3 activity colocalizes with APP cleavage products and amyloid-β in senile plaques.[25]

APP is expressed in several areas of the central nervous system, including the RGCs, and is packaged in small transport vesicles for rapid anterograde transport in the optic nerve to the plasma membranes in axons, dendrites, and synapses.[26] It plays a role in synaptic homeostasis.[27–29] Synaptic dysfunction in AD is associated with deficient glutamate transport function and susceptibility to excitotoxic injury,[30,31] findings also noted in glaucoma.[32] RGC death in glaucoma seems to share similarities with other chronic neurodegenerations. Because caspases participate in apoptosis and APP is strongly expressed in RGCs,

we examined the involvement of caspase activation and abnormal APP processing in experimental models of rat glaucoma.

METHODS

All animal procedures were approved and supervised by the Institutional Animal Care and Use Committees of the Johns Hopkins University School of Medicine and the University of Texas Health Science Center at San Antonio and adhered to the tenets of the Declaration of Helsinki and the ARVO Statement for the Use of Animals in Ophthalmic and Vision Research.

Rat Optic Nerve Transections

Adult brown Norway rats (n = 15, 225–275 g; Charles River, Cambridge, MA) were anesthetized by intraperitoneal injection of ketamine and xylazine (50 mg/kg and 5 mg/kg body weight, respectively). The eyes were also topically anesthetized with proparacaine hydrochloride 1% drops. The conjunctiva and underlying Tenon capsule were incised in the superior temporal quadrant of the left eye. The optic nerve dura was exposed and incised, avoiding the central retinal artery and vein. The optic nerve was transected 2 mm posterior to the globe. Animals with retinal opacity detected by planar ophthalmoscopy were assumed to have had ischemia and were excluded from the study. Erythromycin ointment was applied to the transected eye. The nonsurgical eye served as the control. Five groups (each consisting of three rats) were killed at each of the following time points after transection: 10 minutes, 1 hour, 6 hours, 1 day, and 5 days. All transected eyes were used for RNase protection assays (RPAs).

Ocular Hypertension Models of Rat Glaucoma

Surgery was performed to obstruct aqueous humor outflow and increase intraocular pressure (IOP) in two ways. The first technique has been described in detail elsewhere.[33] Twenty-four adult brown Norway rats were anesthetized as just described, and a small incision was made in the superior limbal conjunctiva. A pulled glass micropipette attached by polyethylene (PE)-50 tubing to a tuberculin syringe was inserted into a circumferential limbal vein near the cornea, and approximately 0.1 mL of 1.75 M saline was injected into the limbal venous system. The injection was then repeated 2 weeks later. Erythromycin ointment was applied to the surgically treated eye. The nonsurgical eye served as the control. Immediately after sedation and topical anesthesia, IOP was measured in both eyes before surgery and on a weekly basis after surgery, using a calibrated tonometer (Tonopen XL; Mentor, Norwell, MA). Of the 24 rats in which IOP was elevated by saline injection, 8 were used for immunohistochemistry, 13 for Western immunoblot analyses, and 3 for RPAs.

The second technique to increase IOP has been described elsewhere.[34] Major aqueous humor drainage veins of 19 adult brown Norway rats were treated with diode laser (Coherent, Palo Alto, CA). Between 50 and 70 spots were applied over 270° of the limbus (power, 1 W; duration, 0.2 seconds; spot size, 50 μm; wavelength, 522 nm), and the limbal area was similarly re-treated 2 weeks later. IOP was measured in both eyes before surgery and on a weekly basis after surgery. Of the 19 rats in which IOP was elevated by laser treatment, all were used for immunohistochemistry.

The degree of IOP exposure in each ocular hypertensive eye was estimated by first integrating IOP over time in the hypertensive eye (expressed in units of mm Hg-days), then subtracting the IOP–time integral from that in the control eye. This IOP–time integral difference has shown a dose–response effect of pressure on optic nerve axon loss, with a threshold for axon loss at a value of approximately 200 mm Hg-days.[35] IOP exposure was also estimated by noting the highest (peak) IOP difference between hypertensive and control eyes. Optic nerve axon loss was calculated as a percentage of axons lost in the hypertensive eyes compared with the paired control eyes.

Optic Nerve Axon Counts

After enucleation, optic nerves were removed from the globe and fixed in cold 4% paraformaldehyde in 0.1 M phosphate buffer (pH 7.2). The nerves were rinsed in Sorenson phosphate buffer (pH 7.2), postfixed in 2% osmium tetroxide in Sorenson phosphate buffer, dehydrated in alcohol, and embedded in epoxy resin. One-micrometer cross sections of myelinated optic nerves were stained with 1% toluidine blue, and approximately 20% of the total axons are counted using an imaging system (Vidas; Carl Zeiss, Inc., Thornwood, NY).[36] Rats used in the procedures were killed by pentobarbital overdose.

RNase Protection Assay

After deep sodium pentobarbital anesthesia, control and treated eyes of transection-treated and ocular hypertensive rats were quickly enucleated and corneas removed. Retinas were detached by blunt dissection and snap frozen in liquid nitrogen. To obtain sufficient amounts of RNA for RPA, three retinas were pooled from each group (control, ocular hypertensive, and optic nerve axotomy at time points 10 minutes, 1 hour, 6 hours, 1 day, and 5 days after transection). RNA was prepared according to the manufacturer's standard protocols (RNeasy; Qiagen, Inc., Valencia, CA). RPA was performed using a commercial system, according to the manufacturer's standard protocol (RiboQuant Multi-Probe; PharMingen, San Diego, CA). Briefly, a set of templates corresponding to rat apoptosis mRNA sequences were subcloned into pPMG vectors that contained a T7 promoter site (provided by PharMingen). Templates were transcribed with T7 polymerase in the presence of [α-^{32}P]UTP, yielding radiolabeled RNA probes. After DNase treatment, the probe set was purified. The probe set and three sets of 2 μg of each pooled retinal RNA preparation were hybridized overnight at 56°C, sequentially treated with RNase and proteinase K, and purified. The resultant protected probes for each group were electrophoresed and run in triplicate lanes on a denaturing polyacrylamide gel (19:1 acrylamide/bis), imaged, and quantified (PhosphorImager SI and ImageQuant software; Molecular Dynamics, Sunnyvale, CA). To compensate for slight variations in loading and reaction mixture composition, band normalization for each lane was performed relative to its bands of the housekeeping genes glyceraldehyde-3-phosphate dehydrogenase (GADPH) and L32. The RPA experiment was duplicated, and results given for the second run are representative of both runs.

Activated Caspase-3 Immunoblots

Treated and control retinas were obtained from ocular hypertensive rats (n = 8 animals, hypertonic saline model) as described earlier. Retinas were individually sonicated in buffer (10 mM HEPES [pH 7.4], 2 mM EDTA, 0.1% 3-([3-cholamidopropyl]dimethylammonio-2-hydroxy-1-propanesulfonate [CHAPS], 5 mM dithiothreitol [DTT], 1 mM phenylmethylsulfonyl fluoride [PMSF], 10 μg/mL pepstatin A, 10 μg/mL aprotinin, and 20 μg/mL leupeptin). Lysate was boiled for 5 minutes in a water bath and centrifuged at 16,000g for 10 minutes. Protein was quantified using the bicinchoninic acid (BCA) technique (Pierce, Rockford, IL). Retinal proteins (70 μg) were analyzed by SDS-PAGE on a 12% Tris-glycine gel (Bio-Rad, Hercules, CA). Proteins were electroblotted onto a nitrocellulose membrane (Hybond-ECL; Amersham, Arlington Heights, IL). The membrane was fixed in a 25% methanol-10% acetic acid solution for 10 minutes and blocked for 1 hour at room temperature in blocking solution (PBST: phosphate-buffered saline [pH 7.4], 0.1% Tween 20 with 5% wt/vol milk). The blot was washed in PBST and incubated for 1 hour at room temperature in a rabbit polyclonal antibody that preferentially recognizes proteolytically activated caspase-3 (CM1; IDUN Pharmaceuticals, La Jolla, CA; 1:1333 in PBST). After washes in PBST, the blot was incubated in HRP-conjugated anti-rabbit secondary antibody (Amersham; 1:2500 in PBST). The blot was washed again in PBST, immersed in enhanced chemiluminescence (ECL) reagents according to standard protocol (Amersham), and exposed to x-ray film. Densitometry was performed as described for RPA. Densitometry of p20 and p30 bands from eight ocular hypertensive and eight control p20 bands was

performed (ImageQuant; Molecular Dynamics). To control for loading artifacts, the p20-to-p30 band ratio was calculated for each of the ocular hypertensive and control eyes and the groups tested for significance using the paired Student's *t*-test.

Activated Caspase-3 Colorimetry

Treated and control retinas were obtained from eight ocular hypertensive rats (hypertonic saline model) as described earlier. Colorimetry was performed according to the manufacturer's protocol (R&D Systems, Inc., Minneapolis, MN). Retinas were individually homogenized in lysis buffer and protein levels quantified using the BCA technique. One hundred micrograms of protein lysate from each pair of ocular hypertensive and control retinas were tested for caspase activity by the addition of the caspase-3–caspase-7–specific peptide, DEVD, conjugated to the color reporter molecule *p*-nitroanilide (DEVD-pNA). After incubation for two hours at 37°C, the individual colorimetric reactions were spectrophotometrically quantified at a wavelength of 405 nm (spectrophotometer model DU640; Beckman, Fullerton, CA). Controls included reactions with no protein lysate and no DEVD-pNA substrate. Results from the eight ocular hypertensive and eight control retinas were averaged and tested for significance with the paired Student's *t*-test.

Immunohistochemistry

For immunohistochemistry, both eyes of 27 adult brown Norway rats were studied after production of unilateral experimental ocular hypertension ($n = 8$ with hypertonic saline model; $n = 19$ with laser model). Eyes were immersion fixed in 4% paraformaldehyde-5% sucrose for 1 hour and cryopreserved in a 1:1 solution of 20% sucrose-optimal temperature cutting (OCT) compound (Sakura Finetek USA, Torrance, CA).[37] Optic nerves were removed and fixed in 4% paraformaldehyde before the globe was fixed. Retinal sections within 1.5 mm of the optic disc that included the central retina measuring 8 μm in thickness were collected onto slides (Superfrost Plus; Fisher Scientific, Pittsburgh, PA). Retinal sections were immunolabeled by a modified streptavidin-biotin peroxidase technique.[38] After methanol fixation, endogenous tissue peroxidase activity was quenched with 3% H_2O_2. The sections were blocked with 2% normal goat serum in PBS, followed by blocking with ABC avidin-biotin blocker (Vector Laboratories, Burlingame, CA). The sections were incubated overnight at 4°C with antibodies detecting the p20 subunit of activated caspase-3 (CM1, IDUN Pharmaceuticals; 1:3000; R&D Systems, Inc., 1:200; and Pharmingen, 1:500), the caspase-3 C-terminal cleavage product of APP (ΔC-APP, 1:600; Merck-Frosst, Montreal, Quebec, Canada), amyloid-β (R1282, 1:800; kindly furnished by Dennis Selkoe, Harvard Medical School, Boston, MA), and full-length proenzyme and activated caspase-8 (SK441 and SK440 respectively, 1:800 and 1:750; kindly furnished by Smith-Kline Beecham, Philadelphia, PA). After washing, the sections were incubated with secondary biotin-conjugated goat anti-rabbit IgG (1:500 dilution; Kierkegaard & Perry, Gaithersburg, MD), washed again, and incubated with peroxidase-labeled streptavidin (1:500 dilution; Kierkegaard & Perry). After incubation in 3-amino-9-ethylcarbazole (AEC; Sigma, St. Louis, MO), sections were mounted in Kaiser glycerol jelly and imaged by Nomarski optics (Axioskop; Carl Zeiss, Inc.). Antibody control experiments included nonimmune serum and exclusion of primary antibody. Two graders, masked to the protocol for each specimen, graded the presence or absence of antibody labeling independently. Differences in grading were adjudicated before unmasking the slides.

APP and Amyloid-β Immunoblot Analyses

Treated and control retinas were obtained from ocular hypertensive rats ($n = 5$ animals, hypertonic saline model), as described earlier. Retinal proteins were individually prepared and quantified as for immunohistochemistry. Retinal proteins (60 μg) were analyzed by SDS-PAGE on a 12.5% Tris-HCl gel (Bio-Rad). Proteins were electroblotted onto a polyvinylidene difluoride (PVDF) membrane (Bio-Rad) and blocked as for immunohistochemistry. The blot was incubated over-

night at 4°C in a mouse monoclonal antibody that recognizes full-length APP (22c11, 1:2000 in PBST; Chemicon, Temecula, CA), followed by incubation for 1 hour at room temperature in HRP-conjugated anti-mouse secondary antibody (1:1000 in PBST; Dako, Carpinteria, CA). The blot was immersed in ECL reagents and exposed to x-ray film. Densitometry was determined for the five ocular hypertensive and five control 22c11 bands. The blot was then stripped for 30 minutes at 55°C in 100 mM 2-mercaptoethanol, 2% SDS, and 62.4 mM Tris-HCl (pH 6.7) and washed in PBST. The blot was incubated overnight at 4°C in a mouse monoclonal antibody that recognizes amino acids 17-24 of rat amyloid-β (4G8, 1:5000 in PBST; Senetek, Napa, CA), incubated in HRP-conjugated anti-mouse secondary antibody (1:1000 in PBST; Dako), immersed in ECL reagents, and exposed to x-ray film. Densitometry was determined for the five ocular hypertensive and five control 4G8 bands. Results from ocular hypertensive and control groups were tested for significance using paired Student's *t*-tests.

RESULTS

Upregulation of Apoptosis-Related Genes by RPA

To understand changes in expression of apoptosis-related genes in glaucoma, we examined rats after RGC injury using an RPA to measure mRNA levels for various apoptosis-related genes (Fig. 1). To compare retinal gene expression between various models of RGC degeneration, we studied retinal mRNAs in an ocular hypertensive model of glaucoma and at time points in the first week after optic nerve transection, during which 50% of RGCs would be expected to die.[39] Rat total RNA was isolated and pooled for each group (see the Methods section) to produce enough RNA for the RPA assay. The three ocular hypertensive eyes were exposed to elevated IOP for 5 weeks, with a mean IOP–time integral difference of 100 mm-days (range, 14–158). The mean peak IOP difference between the three pairs of hypertensive and control eyes was 12.0 mm (range, 10–14). This mild degree of pressure exposure was chosen to maximize the induction of apoptosis-related genes while minimizing RGC mRNA loss. Because ocular tissue was used for RNA isolation, optic nerve axon loss was not quantified for the ocular hypertensive or transected eyes.

Bcl-x_L mRNA was expressed at a higher level than that of bcl-2 in all retinas examined, consistent with results in a prior study.[40] Caspase-1 mRNA was not observed in the retinas of control eyes or in those after optic nerve transection or with ocular hypertension. Caspase-2 and -3 and bax mRNAs were expressed at higher levels in transected and ocular hypertensive retinas when compared with control retina. Also, caspase-3 mRNA was expressed at a level comparable to bcl-x_L and higher than caspase-2 and -1. Densitometry of individual mRNAs in the rat retina RPA experiment (Fig. 2) showed that both bcl-x_L and caspase-3 were expressed constitutively in normal retina and were rapidly upregulated after transection, reaching a maximum at 6 hours after transection (Fig. 2). In glaucoma retina, the levels of bcl-x_L and caspase-3 mRNA were also increased. Both bcl-x_L and caspase-3 mRNA levels in ocular hypertensive eyes were higher than the peak expression 6 hours after optic nerve transection. Normalization of band densitometry was also repeated using the L32 bands, and produced results similar to those seen with GAPDH normalization (data not shown).

Activated Caspase-3 Levels

IOP was measured weekly for 15 weeks from eight eyes in which hypertension was produced by the hypertonic saline injection method and from the paired control eyes. The average IOPs for the glaucoma and control groups are shown with the SEM (error bars) in Figure 3. The mean IOP–time integral difference in these eight rats was 255 ± 40 mm-days (range,
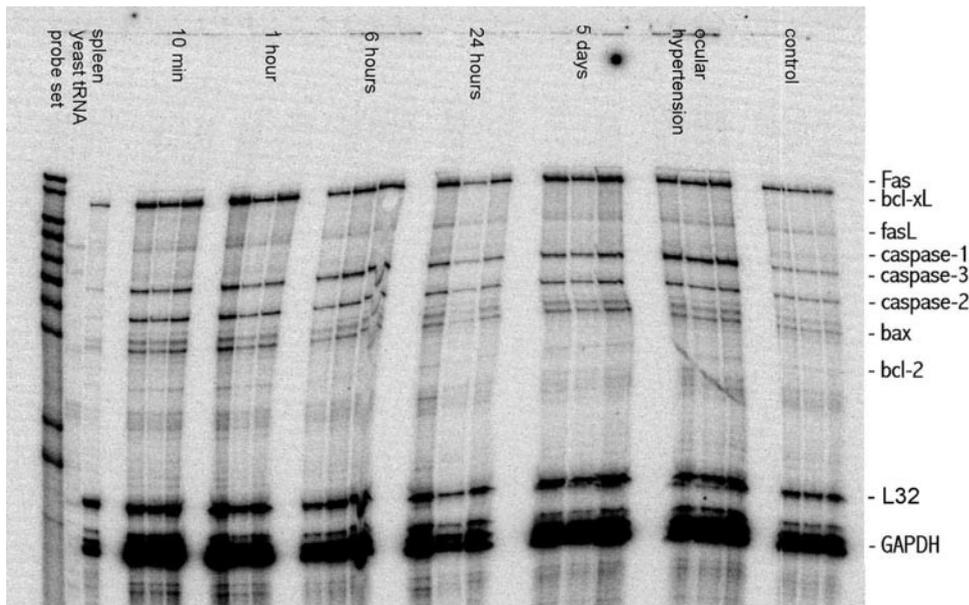
FIGURE 1. RPA of rat retina. The RNA probe set (in order of decreasing size) included probes to Fas receptor; bcl-X$_L$; fas ligand (fasL); caspase-1, -3, and -2; bax; bcl-2; and GAPDH. Samples run included the probe set, controls consisting of yeast tRNA and rat spleen; rat retinas harvested 10 minutes, 1 hour, 6 hours, 24 hours, and 5 days after transection; rat ocular hypertensive retina; and control rat retina. Total RNA from each group ($n = 3$ per group) was pooled, and separate 2-μL aliquots were run in triplicate lanes.

85–465); the mean peak IOP difference between hypertensive and control eyes was 9.5 ± 1.3 mm Hg (range, 6–15). This moderate degree of pressure exposure was chosen to maximize the activation of caspase-3 in RGCs. Mean optic nerve axon loss was $63.4\% \pm 13.7\%$ (range, 0–110) for these eight ocular hypertensive eyes.

The immunoblots of rat retinal protein from the eight pairs of ocular hypertensive and control eyes were probed with the CM1 antibody that preferentially recognized the activated p20 subunit of caspase-3, as well as the precursor p32 band (Fig. 4). Given the similarity of p32 band expression between hypertensive and control eyes, the change in ratio of p20 to p32 bands was calculated for each eye. When compared with direct analysis of p20 bands, using the p20-p30 ratios more accurately reflected increases in caspase-3 processing and eliminated gel-loading artifacts. Caspase-3 activation, as judged by p20-p30 band ratios, was significantly higher in the eight ocular hypertensive retinas than in the matched control specimens (0.87 ± 0.15 vs. 0.28 ± 0.05, mean $\pm$ SEM; $P < 0.013$, paired Student's *t*-test; Fig. 5A). As a confirmatory test, combined caspase-3 and -7 activation was quantified by colorimetric assay. Ocular hypertensive retinas had significantly higher caspase-3 and -7 activity than did control retinas (532 ± 65 vs. 185 ± 18, mean $\pm$ SEM; $P < 0.009$, paired *t*-test; Fig. 5B).

Immunohistochemical Evidence

Immunolabeling was performed in 27 experimental ocular hypertensive rats. Of the ocular hypertensive eyes, 19 underwent laser-induced IOP elevation, and 8 underwent hypertonic saline-induced IOP elevation. The mean duration of observation from production of elevated IOP to death for the laser model was 5 weeks (range, 8–46 days). The eight rats in the hypertonic saline injection model were observed for 3 weeks after IOP elevation. In comparing the course of ocular hypertension and its effects in the two models, there were some slight differences. The mean IOP–time integral difference for the laser group was 58 ± 52 mm Hg-days (SD; range, 5–234) and for the saline injection group was 23 ± 4 mm Hg-days (range, 17–27). The mean peak IOP difference between hypertensive and control eyes for the laser group was 16.3 ± 5.5 mm Hg (SD; range, 8–26), and for the saline injection group 14.4 ± 3.0 mm Hg (range, 9–18). The low integral values derive from the fact that the hypertensive

eyes had higher IOP early in their course, with a later decline. However, the mean peak IOP differences between the laser and saline groups were similarly elevated. These comparatively short durations were chosen to study the effects of chronic IOP exposures of less than 100 mm Hg-days, at points before the death of large numbers of RGCs. The loss of RGCs as measured by optic nerve axon counts (mean $\pm$ SD) was slightly, but not significantly, greater in the laser group than in the hypertonic saline group ($12\% \pm 16\%$ versus $0\% \pm 20\%$; $P = 0.13$). However, it would not be expected that large numbers of RGCs would die in the short time frame of these experiments. In fact, we purposely studied the period before major cell death so that loss of RGCs was not a factor in determining differences among groups.

Labeling for activated caspase-3 with the CM1 antibody was detected in the RGC layer of ocular hypertensive eyes significantly more than in normal eyes (Figs. 6A, 6B). The masked graders designated each slide as positive or negative for labeling with CM1. With this method (Table 1), 85% were graded as positive among ocular hypertensive eyes, and 41% were positive among the control eyes. The presence of positive labeling in control eyes may be explained by the fact that the CM1 antibody also recognizes the inactive p32 form of caspase-3, as seen in the CM1 Western blot. There was no difference in the rate of positivity between ocular hypertensive eyes from the two different models.

We obtained even more striking differences between ocular hypertensive and normal eyes with a second marker for caspase-3 activation, an antibody against the carboxyl-terminal caspase-3 cleavage product of APP (ΔC-APP, Figs. 6C, 6D). Slides (Table 1) showed significant elevation of ΔC-APP immunolabeling 3.5 times more often in ocular hypertensive (52%) than in control (15%) eyes. In a multivariate regression model with positive labeling for ΔC-APP as the independent variable, RGC loss and ocular hypertensive duration were significant dependent variables, adjusting for IOP exposure (both $P < 0.03$, 95% confidence interval of RGC loss: 0.18–2.33; and duration in weeks: 0.02–0.35).

Activated Caspase-8 and Amyloid-β Levels

Labeling of the inactive proenzyme form of caspase-8 was uniformly present in ocular hypertensive and control retinas
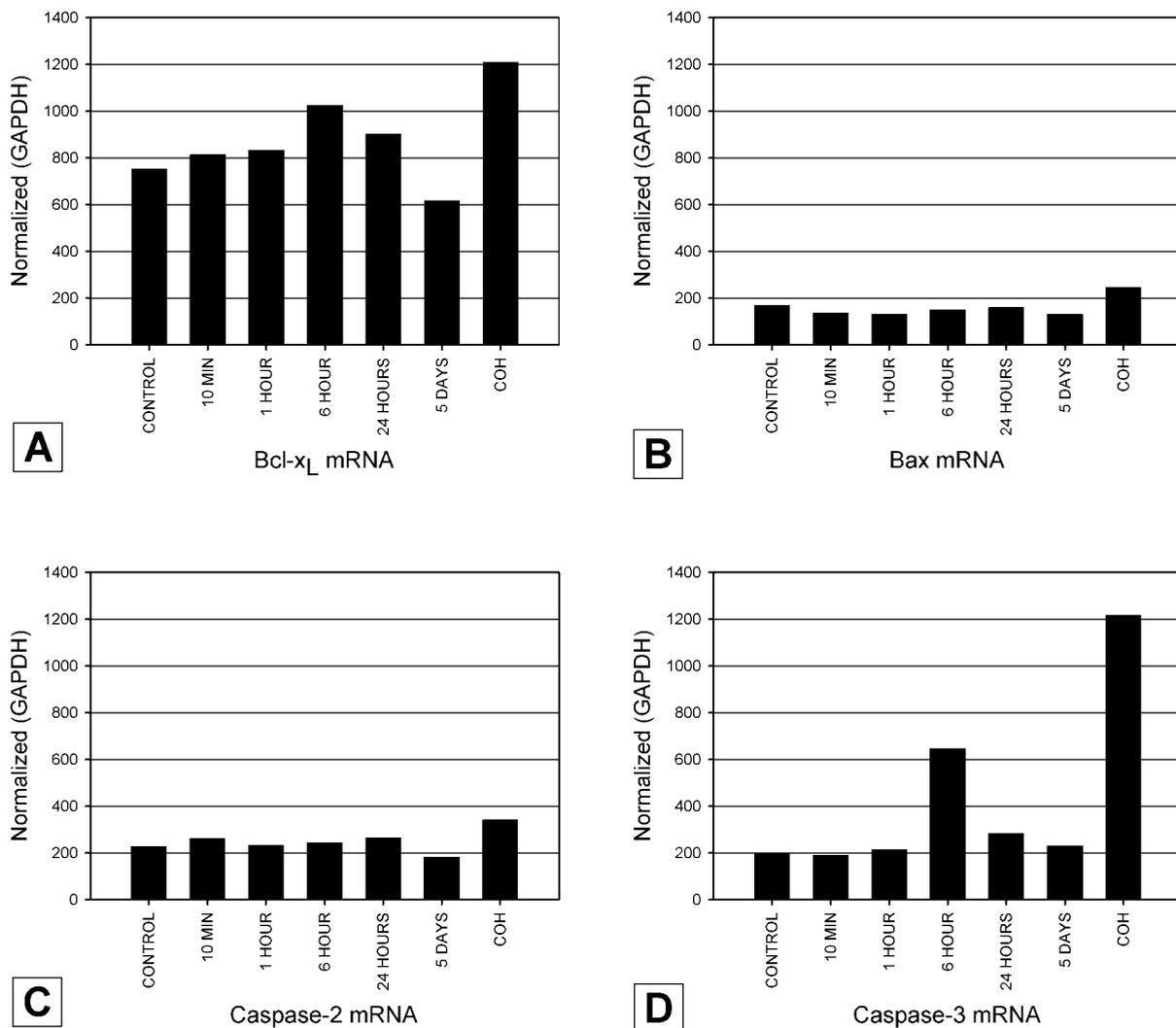
FIGURE 2. Densitometry of RPA bands. The individual bands for the protected probes bcl-X_L (**A**), bax (**B**), caspase-2 (**C**), and caspase-3 (**D**) were quantified and normalized to the corresponding GAPDH bands. GAPDH bands were set at a value of 10^5 for normalization. The normalized values for each probe are displayed for control rat retina; rat retinas at 10 minutes, 1 hour, 6 hours, 24 hours, and 5 days after transection; and rat chronic ocular hypertensive (COH) retina.

(Figs. 7A, 7B), and the difference was not statistically significant (Table 1). Where it was detected, inactive caspase-8 labeling was strongest in the RGC layer, with moderate staining in the inner and outer nuclear layers. However, immunolabeling of the activated form of caspase-8 was graded as much heavier in the RGC layer of ocular hypertensive eyes than in control eyes (Figs. 7C, 7D). A masked reading of slides (Table 1) showed statistically significant elevation of activated caspase-8 immunolabeling in ocular hypertensive eyes (81%) when compared with control eyes (4%). The heavier labeling for activated caspase-8 was present in both ocular hypertension models. Control sections using no primary antibody also showed negligible background staining (data not shown).

Increased amyloid-β immunolabeling was noted in the RGC layer of ocular hypertensive retinas (Figs. 7E, 7F) and was heavier in both the laser and saline injection models to a similar degree. A masked reading of slides (Table 1) showed striking and statistically significant elevation of amyloid-β immunolabeling in ocular hypertensive eyes (96%) when compared with control eyes (0%). Occasional labeling of cells was also seen in the inner nuclear layer of ocular hypertensive retinas.
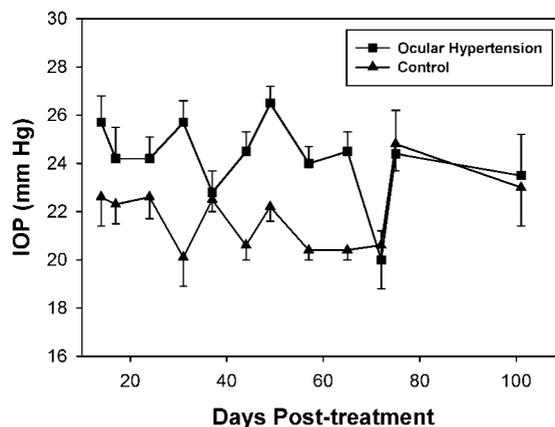

FIGURE 3. Rat intraocular pressure (IOP) time course. The IOP time course over approximately 15 weeks is averaged for the eight pairs of rat eyes used in the activated caspase-3 immunoblot and colorimetry experiments. The group mean ocular hypertensive IOPs were elevated over control IOPs. Error bars, SEM.
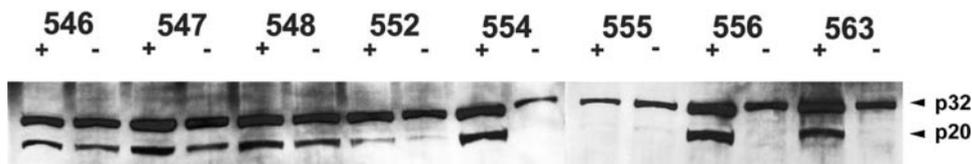
FIGURE 4. Activated caspase-3 immunoblots. Western immunoblot of retinal protein from eight pairs of ocular hypertensive (+) and control (−) eyes using CM1 antibody shows upregulation of the activated caspase-3 p20 band (1:1333 dilution) in hypertensive retinas.

Abnormal APP Processing

To further delineate the immunohistochemical evidence of abnormal processing of APP in rat ocular hypertension, we performed Western blot analysis on retinal protein obtained from five Norway brown rats with unilateral ocular hypertension. The five ocular hypertensive eyes were exposed to elevated IOP for 12 weeks, with a mean IOP–time integral difference of 104 ± 32 mm Hg-days (SEM; range, 8–231). The mean peak IOP difference between the five pairs of hypertensive and control eyes was 5.2 ± 1.1 mm Hg (SEM; range, 2–9). Because we had shown that caspases were activated early in the course of chronic IOP elevation, we chose a mild degree of pressure exposure to maximize caspase activity and abnormal APP processing. Optic nerve axon loss was not quantified for these five ocular hypertensive eyes.

The blot was probed with antibodies directed against specific epitopes of the APP molecule. The upper (115-kDa) bands (Fig. 8) represent the amount of full-length APP in control (−) and ocular hypertensive (+) rat retinas as measured by the 22c11 antibody. The levels of full-length APP are reduced in the hypertensive retinas when compared with the control retinas. Densitometry of the 115-kDa bands (Fig. 9A) confirmed a statistically significant decrease in full-length APP in the hypertensive retinas when compared with the control retinas ($P <$ 0.015, paired *t*-test). The lower (21-kDa) bands (Fig. 8) represent fragments of APP containing amyloid-β epitopes (4G8 antibody) in control (−) and ocular hypertensive (+) rat retinas. The levels of 21-kDa protein recognized by 4G8 were elevated in hypertensive retinas when compared with control retinas. Densitometry of these 21-kDa bands (Fig. 9B) quantified a statistically significant increase in amyloid-β epitopes in hypertensive retinas when compared with control retinas ($P <$ 0.0001, paired *t*-test).

DISCUSSION

We investigated alterations in the rat retina after the production of ocular hypertension and optic nerve transection, with specific reference to cellular components related to neuronal survival. There was a specific and substantial activation of caspase-3 and caspase-8 in ocular hypertension models of rat glaucoma. This includes evidence that caspase-3 is present in its activated form and one of its known cleavage products, ΔC-APP, is present in RGCs of ocular hypertensive eyes to a substantially greater extent than in normal retinas. Additional findings included increases in the mRNA coding for bax and bcl-x_L, gene products that are known to have opposing roles in neuronal survival. Finally, the decrease in full-length APP levels with a concomitant increase in amyloid-β–containing fragments was another important finding pointing to the role of abnormal APP processing in ocular hypertensive eyes. We propose that these data delineate with greater precision the mechanism by which RGCs die in glaucoma.

We used two different model systems to chronically elevate IOP for durations of 1 to 12 weeks in these experiments. Although these models lead to RGC death in substantially shorter periods than in human glaucoma, similarities between rat and human eyes should show the relevance of rat ocular hypertension to chronic glaucoma in humans. Specifically, assessment of optic nerves in the limbal injection model showed that with shorter or less severe IOP exposures, partial damage had occurred, ranging from 0.5% to 10.4% of the neural area. Optic nerves subjected to the greatest IOP exposures demonstrated axonal damage that involved 100% of the neural area.[33] The two rat ocular hypertensive models used in this study gave consistently similar results, assuring that our experiments were not dependent on one method to increase IOP. However, confirmation of these findings in nonhuman primate and human eyes will be sought.
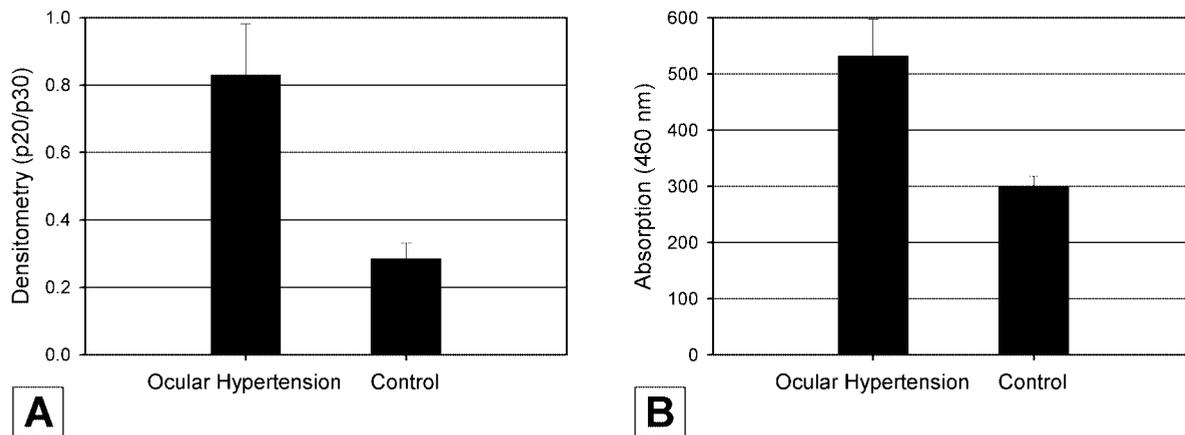
FIGURE 5. Activated caspase-3 densitometry and colorimetry. (**A**) Ocular hypertensive eyes had significantly greater activation of caspase-3 (p20-p30 ratio) by densitometry of CM1 immunoblot (1:1333 dilution; $P <$ 0.013, paired Student's *t*-test). (**B**) Average colorimetry of activated caspase-3 of retinal protein from eight pairs of ocular hypertensive and control eyes shows significantly greater activity in ocular hypertensive eyes ($P <$ 0.009; paired Student's *t*-test). Error bars, SEM.

FIGURE 6. Caspase-3 immunohistochemistry. (**A**) Ocular hypertensive rat retina exposed to 4 weeks of elevated IOP stained with CM1 antibody recognizing activated caspase-3 showed prominent labeling of the GC layer (1:3000 dilution). (**B**) Control rat retina stained with CM1 antibody recognizing activated caspase-3 showed no labeling of the GC layer (1:3000 dilution). (**C**) Definite labeling was seen in the GC layer of the hypertensive rat retina exposed to 4 weeks of elevated IOP stained with ΔC-APP antibody recognizing the activated caspase-3 cleavage product of APP (1:600 dilution). (**D**) No labeling was seen with the ΔC-APP antibody recognizing the activated caspase-3 cleavage product of APP in control rat retina (1:600 dilution). GC, ganglion cell layer; IPL, inner plexiform layer; INL, inner nuclear layer; OPL, outer plexiform layer; ONL, outer nuclear layer; PR, photoreceptor layer. Magnification, ×40; Bar, 40 μm.

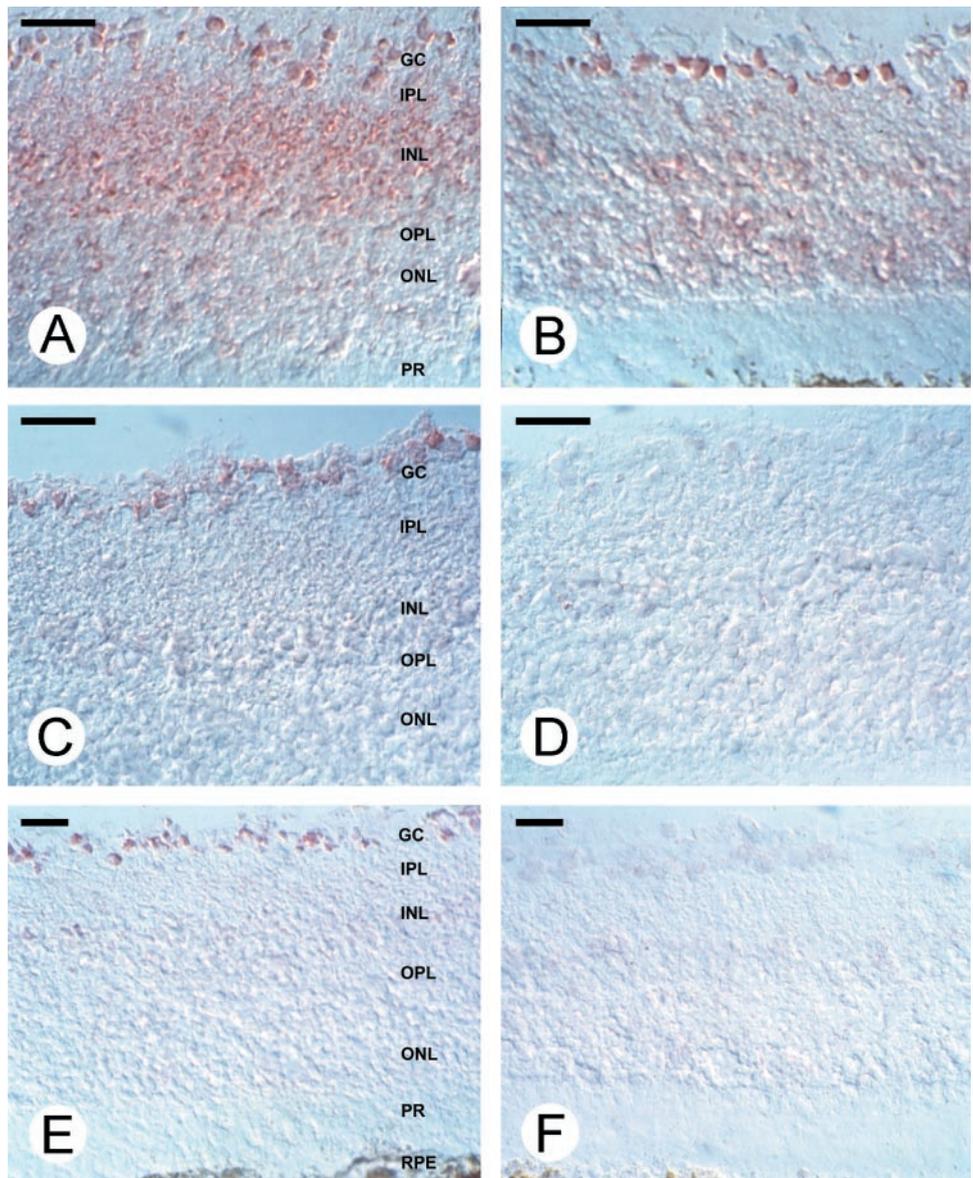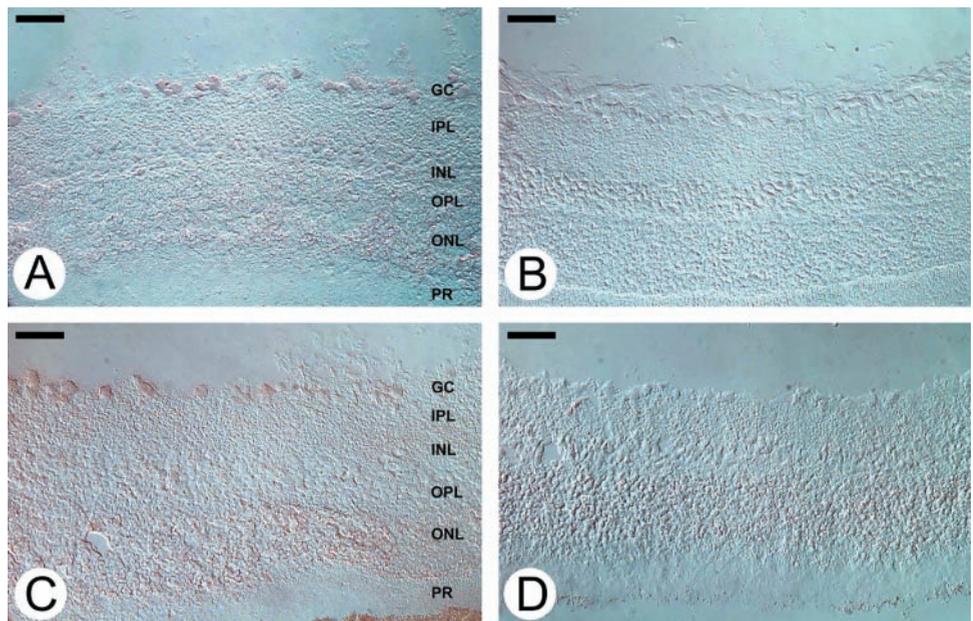FIGURE 7. Caspase-8 and amyloid-β immunohistochemistry. (**A**, **B**) Ocular hypertensive rat retina exposed to 4 weeks of elevated IOP (**A**) and control rat retina (**B**) both showed substantial labeling of GC and INL with antibody recognizing the inactive proenzyme form of caspase-8 (1:800 dilution). (**C**, **D**) Ocular hypertensive rat retina exposed to 4 weeks of elevated IOP (**C**) showed intense GC labeling with antibody recognizing activated caspase-8, whereas control rat retina (**D**) was not stained with this antibody (1:750 dilution). (**E**, **F**) Ocular hypertensive rat retina exposed to 4 weeks of elevated IOP (**E**) showed intense staining of GC with antibody recognizing amyloid-β, whereas control rat retina (**F**) showed no staining (1:250 dilution). Abbreviations are as in Figure 6. Magnification, (**A**–**D**) ×63; (**E**, **F**) ×40. Bar, 40 μm.

TABLE 1. Masked Reading of Immunohistochemistry

	Hypertensive Retina		Control Retina		
Antibody	Ratio	% Positive	Ratio	% Positive	P
Activated caspase-3	23/27	85	11/27	41	0.004*
ΔC-APP	14/27	52	4/27	15	0.013*
Proenzyme caspase-8	25/27	93	26/27	96	0.55
Activated caspase-8	22/27	81	1/27	4	0.0001*
Amyloid-β	22/23	96	0/23	0	0.0001*

Probabilities obtained with χ^2 test.
* Significant at $P < 0.05$.

Previous investigations have shown that RGCs die by apoptosis in rat and monkey glaucoma models and in human glaucoma,[5–7] as well as after optic nerve transection in rabbits[6] and in human ischemic optic neuropathy.[41] These investigations indicate that processes that injure the axon of RGCs at or just behind the eye lead to apoptosis. Evidence favoring apoptosis includes typical histologic features, such as TUNEL-labeling of RGCs and DNA laddering in electrophoretic analysis of retinal digests. We have suggested that RGC death by apoptosis occurs as a direct result of axonal injury and its secondary effects. One important potential consequence for the RGC body of axon injury is disruption of axonal transport, including retrograde delivery of neurotrophins.[12] The obstruction of retrograde transport would clearly occur in optic nerve transection and has been shown to occur in experimental glaucoma.[42] Yet, it is not known what events might be initiated at the level of the RGC body as a result of remote axonal injury. A variety of studies have evaluated RGC responses to axon injury.[40,43,44] It is well known that mammalian RGCs respond to axonal injury by dying, rather than by initiating a successful regenerative response.

Our findings point to at least two plausible pathways by which axonal injury could initiate apoptotic RGC death. The activation of caspase-8 is considered an initiating step in the apoptosis cascade[45] and has been noted in RGC cultures exposed to heat-shock proteins.[46] Apoptosis initiated by caspase-8 involves cell membrane-bound receptors of the tumor necrosis factor (TNF) superfamily, including TNFR, Trail, Fas, and the low-affinity neurotrophin receptor p75NTR. Recent work has demonstrated immunohistochemical evidence of upregulation of both TNFR and ligand TNF-α in human glaucomatous retina.[47] A so-called death domain in the cytoplasmic portion of each receptor recruits adaptor proteins such as FADD. An effector domain of FADD binds to and activates caspase-8, forming an active signaling complex that is known to activate caspase-3 and to induce cell death.[18] The activation of caspase-3 leads to cleavage of the C-terminal cytoplasmic tail of APP, yielding neurotoxic peptide fragments that have been shown to upregulate amyloid-β production in hippocampal neurons.[25,48–52] Thus, we show two steps, caspase-8 and -3 activation, that could represent sequential events in the apoptotic cascade in RGCs during exposure to ocular hypertension.

Our data suggest that a second series of events may contribute to RGC death in rat ocular hypertension and perhaps in human glaucoma. APP is expressed throughout the brain, including the RGCs, playing a central role in neurite outgrowth, synaptogenesis, and cell survival.[27,28] It is also protective against excitotoxicity, by membrane hyperpolarization induced by the activation of cGMP and increased inward K^+ currents.[29] It is known to undergo rapid anterograde transport in the optic nerve.[26] Because glaucoma obstructs not only retrograde but also anterograde axonal transport,[42,53,54] it is conceivable that anterograde blockade causes an increase in retinal APP levels. In neurons, apoptosis can be induced by adenoviral overexpression of APP,[55] and elevated APP levels are known to activate caspase-3, leading to APP cleavage into fragments that upregulate amyloid-β levels.[48,51] Increased amyloid-β potentiates apoptosis in the central nervous system[56] and is capable of activating both caspase-8[57] and -3[58] in primary neuronal cultures. These events could participate in a positive feedback loop, with further caspase-3 activation, APP cleavage, and amyloid-β formation.[59] We believe there is a similar situation in rat ocular hypertension, because we have detected increased retinal levels of activated caspase-3, APP fragments, and amyloid-β. In this scenario, RGCs may ultimately die from amyloid-β cytotoxicity, caspase activation, increased vulnerability to excitotoxic insults, and loss of synaptic homeostasis. We have also shown increased amounts of amyloid-β-containing 21-kDa fragments of APP in rat ocular hypertension. These 21-kDa APP fragments have been noted to be up-regulated in cerebral vasculature in AD and Down's syndrome brains.[60,61] This raises the intriguing possibility that amyloid deposition may contribute to vascular disease in glaucoma. We intend further study of the expression of APP and amyloid-β in the microvasculature of the retina and optic nerve head in the rat ocular hypertension model of glaucoma.

Glaucoma and AD are both chronic neurodegenerative conditions, and features of neuronal dysfunction in AD suggest parallels to those detected in RGCs in glaucoma. Caspase-3 activity has been colocalized with abnormal neurofilament triplet protein (NFT) production in the hippocampus of AD brains.[62] NFTs have also been localized to large RGCs.[63,64] It is interesting that those investigators who detect a loss of RGCs in AD indicate that larger diameter RGCs are selectively lost, a feature recently confirmed to be the case in human glaucoma.[65] However, the characteristic neuropathologic findings in AD—NFTs and deposition of amyloid in neuritic plaques[66]—have not been found in the retina of human glaucomatous eyes.[4] Synaptic dysfunction in AD is associated with caspase activity[67] and deficient glutamate transport function,[30,31] leading to increased susceptibility to excitotoxic injuries. Synaptic dysfunction has been implicated in glaucoma, as loss of lateral geniculate neurons occurs in magnocellular and parvocellular layers in glaucomatous monkeys.[68] Excitotoxic triggers, such as elevated glutamate[13,69] and nitric oxide synthase upregulation with reactive oxygen species formation,[16] have been implicated in glaucoma, as they have in AD.[70] There is evidence that RGCs die in AD at a rate greater than in normal aging[71–75]; however, others investigators have been unable to confirm these findings.[76]

Further parallels between our findings in RGCs and known events in AD include increases in amyloid-β and the cleavage of its precursor molecule APP. APP mutations lead to inherited,
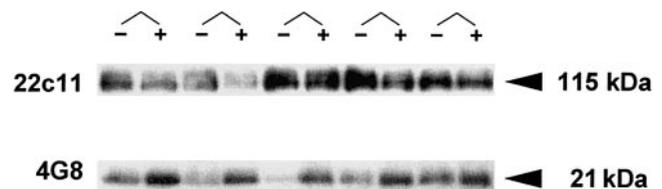
FIGURE 8. APP and amyloid-β immunoblots. Immunoblot of retinal protein from control (−) and ocular hypertensive (+) retinas, using 22c11 antibody recognizing full-length APP (1:2000 dilution; 115-kDa band, *top*); immunoblot of the same membrane stripped and reprobed with 4G8 antibody recognizing amino acids 17-24 of amyloid-β (1:5000 dilution; 21-kDa band, *bottom*). Lower levels of 115-kDa protein were seen in hypertensive eyes than in control eyes, whereas higher levels of 21-kDa protein were seen in hypertensive eyes than in control eyes.

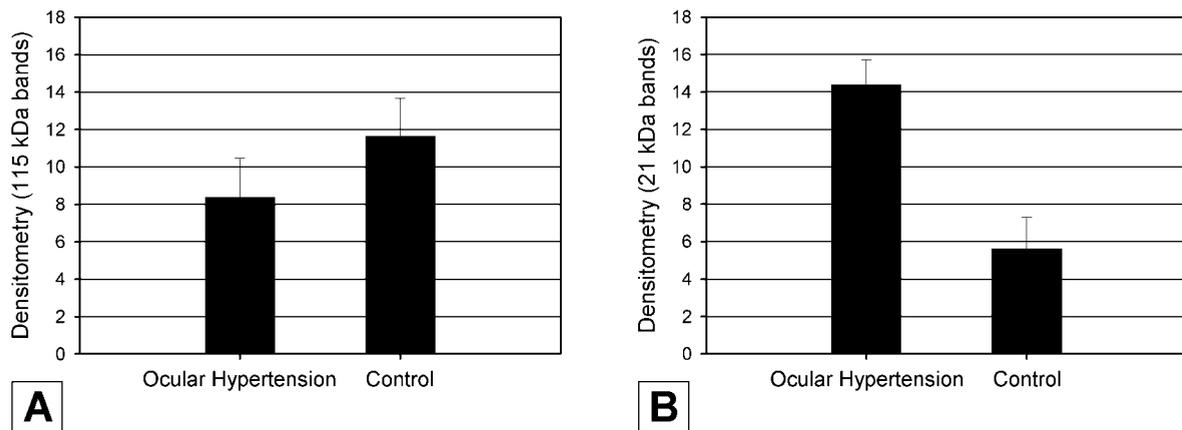**FIGURE 9.** APP and amyloid-β densitometry. (**A**) Comparison of average densitometry of 115-kDa bands using 22c11 antibody showed that ocular hypertensive retinas expressed significantly less full-length APP than did control retinas ($P < 0.015$, paired *t*-test). (**B**) Comparison of average densitometry using 4G8 antibody recognizing amino acids 17-24 of amyloid-β showed that ocular hypertensive retinas expressed significantly more 21-kDa protein than did control retinas ($P < 0.0001$, paired *t*-test). Error bars, SEM.

early-onset forms of AD associated with elevated amyloid-β production.[77,78] Recent research using neuronal cell cultures suggests that increased amyloid-β production plays a central role in the apoptotic death of neurons in AD.[79–81] Transgenic mice that overexpress amyloid-β show abnormal neuronal apoptosis.[74] Exposure of cultured cortical neurons to sublethal levels of amyloid-β suppressed both activation of cAMP-response element-binding protein (CREB) and expression of brain-derived neurotrophic factor (BDNF) mRNA.[82] As our immunohistochemistry results indicate, amyloid-β labeling appears to be intracellular, implying upregulation of soluble amyloid-β, rather than the insoluble amyloid fibrils seen in plaques. Soluble intracellular amyloid-β has been increasingly implicated in the pathogenesis of AD.[83,84]

The classic view of apoptosis holds that once caspase activation initiates programmed cell death, the cell will die within 1 to 2 days. Our results contradict this view, in that we detect caspase activation in most RGCs, even when exposed to short durations of elevated IOP in which RGC axon loss is minimal. The fact that caspase activation in the ocular hypertensive rat model does not immediately kill all RGCs within 2 days represents another parallel with chronic neurodegenerations such as AD. Recent work in AD brains has shown that chronic caspase activation induces a slow, apoptosis-like degenerative process that differs from rapid classic apoptosis.[85] Fodrin, a major cytoskeletal protein also involved in axonal transport,[86] is a substrate for caspase-3 cleavage.[87] Cleaved fodrin was found in a large number of viable neurons in association with NFT formation, suggesting that caspases are chronically activated in AD before neuronal death occurs.[62] The decades-long life span of RGCs implies an inherent ability to resist chronic insults, perhaps by implementing survival mechanisms, including upregulation of endogenous apoptosis inhibitors such as bcl-2 or XIAP,[88,89] or downregulation of apoptosis inducers such as Diablo/Smac.[90,91] As in AD, glaucoma may involve lower levels of caspase activation that do not immediately induce cell death but result in delayed apoptosis that renders them vulnerable to oxidative stress.[92] Paradoxically, a protracted course of caspase activation in glaucoma may be beneficial, in that the window for intervention with caspase inhibitors may be longer than previously thought.

Three therapeutic approaches to mitigation of RGC death in experimental rat glaucoma have been reported. In a vein-cautery model of ocular hypertension,[5] peripheral RGCs were lost at a lower rate when treated with aminoguanidine, an inhibitor of inducible nitric oxide synthase.[93] In the same

vein-cautery model, there was increased RGC survival with the use of either the *N*-methyl-D-aspartate (NMDA) receptor antagonist MK-801[94] or a combination of BDNF and free radical scavenger.[95] Although these models lead to RGC death in substantially shorter periods than seen in human glaucoma, the relevance of the rat models is suggested by important similarities to human glaucoma, including axon injury at the optic nerve head and specific loss of RGCs without death of other retinal elements.

Our results indicate a potential role for caspase inhibition in the treatment of glaucoma, in that significant delay of RGC apoptosis has been demonstrated after optic nerve transection in rats using cell-permeable aldehyde-ketone-amino acid caspase inhibitors[96] or adenoviral delivery of p35 and crmA.[97] Our findings also point to similarities in molecular cell death mechanisms between glaucoma and AD, raising the possibility that neuroprotective strategies currently used to treat AD may have utility in treating human glaucoma. By delineating the operative steps that occur in the apoptotic cascade in glaucoma, the specific inhibitions that are likely to be successful can best be determined.

References

1. Leske MC. The epidemiology of open angle glaucoma. *Am J Epidemiol.* 1983;118:116–191.
2. Tielsch JM, Sommer A, Katz J. Racial variations in the prevalence of primary open-angle glaucoma: The Baltimore Eye Survey. *JAMA.* 1991;266:369–374.
3. Quigley HA. Number of people with glaucoma worldwide. *Br J Ophthalmol.* 1996;80:389–393.
4. Quigley HA, Green WR. The histology of human glaucoma cupping and optic nerve damage: clinicopathologic correlation in 21 eyes. *Ophthalmology.* 1979;86:1803–1830.
5. Garcia-Valenzuela E, Shareef S, Walsh J, Sharma SC. Programmed cell death of retinal ganglion cells during experimental glaucoma. *Exp Eye Res.* 1995;61:33–44.
6. Quigley HA, Nickells RW, Kerrigan LA, Pease ME, Thibault DJ, Zack DJ. Retinal ganglion cell death in experimental glaucoma and after axotomy occurs by apoptosis. *Invest Ophthalmol Vis Sci.* 1995;36:774–786.

7. Kerrigan LA, Zack DJ, Quigley HA, Smith SD, Pease ME. TUNEL-positive ganglion cells in human primary open-angle glaucoma. *Arch Ophthalmol.* 1997;115:1031–1035.

8. Nickells RW. Apoptosis of retinal ganglion cells in glaucoma: an update of the molecular pathways involved in cell death. *Surv Ophthalmol.* 1999;43(suppl 1):S151–S161.

9. Quigley HA, Anderson DR. Distribution of axonal transport blockade by acute intraocular pressure elevation in the primate optic nerve head. *Invest Ophthalmol Vis Sci.* 1977;16:640–644.

10. Quigley HA, Guy J, Anderson DR. Blockage of rapid axonal transport: effect of intraocular pressure elevation in primate optic nerve. *Arch Ophthalmol.* 1979;97:525–531.

11. Quigley HA, Flower RW, Addicks EM, McLeod DS. The mechanism of optic nerve damage in experimental acute intraocular pressure elevation. *Invest Ophthalmol Vis Sci.* 1980;19:505–517.

12. Pease ME, McKinnon SJ, Quigley HA, Kerrigan-Baumrind LA, Zack DJ. Obstructed axonal transport of BDNF and its receptor TrkB in experimental glaucoma. *Invest Ophthalmol Vis Sci.* 2000;41:764–774.

13. Dreyer EB, Zurakowski D, Schumer RA, Podos SM, Lipton SA. Elevated glutamate levels in the vitreous body of humans and monkeys with glaucoma. *Arch Ophthalmol.* 1996;114:299–305.

14. Tezel G, Seigel GM, Wax MB. Autoantibodies to small heat shock proteins in glaucoma. *Invest Ophthalmol Vis Sci.* 1998;39:2277–2287.

15. Osborne NN, Ugarte M, Chao M, et al. Neuroprotection in relation to retinal ischemia and relevance to glaucoma. *Surv Ophthalmol.* 1999;43(suppl 1):S102–S128.

16. Neufeld AH. Nitric oxide: a potential mediator of retinal ganglion cell damage in glaucoma. *Surv Ophthalmol.* 1999;43(suppl 1):S129–S135.

17. Tewari M, Quan LT, O'Rourke K, et al. Yama/CPP32 beta, a mammalian homolog of CED-3, is a CrmA-inhibitable protease that cleaves the death substrate poly(ADP-ribose) polymerase. *Cell.* 1995;81:801–809.

18. Enari M, Hug H, Nagata S. Involvement of an ICE-like protease in Fas-mediated apoptosis. *Nature.* 1995;375:78–81.

19. Marks N, Berg MJ. Recent advances on neuronal caspases in development and neurodegeneration. *Neurochem Int.* 1999;35:195–220.

20. Petersen A, Mani K, Brundin P. Recent advances on the pathogenesis of Huntington's disease. *Exp Neurol.* 1999;157:1–18.

21. Morrison BM, Hof PR, Morrison JH. Determinants of neuronal vulnerability in neurodegenerative diseases. *Ann Neurol.* 1998;44:S32–S44.

22. Loetscher H, Deuschle U, Brockhaus M, et al. Presenilins are processed by caspase-type proteases. *J Biol Chem.* 1997;272:20655–20659.

23. Kim TW, Pettingell WH, Jung YK, Kovacs DM, Tanzi RE. Alternative cleavage of Alzheimer-associated presenilins during apoptosis by a caspase-3 family protease. *Science.* 1997;277:373–376.

24. Lu DC, Rabizadeh S, Chandra S, et al. A second cytotoxic proteolytic peptide derived from amyloid beta- protein precursor. *Nat Med.* 2000;6:397–404.

25. Gervais FG, Xu D, Robertson GS, et al. Involvement of caspases in proteolytic cleavage of Alzheimer's amyloid- beta precursor protein and amyloidogenic A beta peptide formation. *Cell.* 1999;97:395–406.

26. Morin PJ, Abraham CR, Amaratunga A, et al. Amyloid precursor protein is synthesized by retinal ganglion cells, rapidly transported to the optic nerve plasma membrane and nerve terminals, and metabolized. *J Neurochem.* 1993;61:464–473.

27. Moya KL, Benowitz LI, Schneider GE, Allinquant B. The amyloid precursor protein is developmentally regulated and correlated with synaptogenesis. *Dev Biol.* 1994;161:597–603.

28. Masliah E. Mechanisms of synaptic dysfunction in Alzheimer's disease. *Histol Histopathol.* 1995;10:509–519.

29. Morimoto T, Ohsawa I, Takamura C, Ishiguro M, Nakamura Y, Kohsaka S. Novel domain-specific actions of amyloid precursor protein on developing synapses. *J Neurosci.* 1998;18:9386–9393.

30. Li S, Mallory M, Alford M, Tanaka S, Masliah E. Glutamate transporter alterations in Alzheimer disease are possibly associated with abnormal APP expression. *J Neuropathol Exp Neurol.* 1997;56:901–911.

31. Tominaga K, Uetsuki T, Ogura A, Yoshikawa K. Glutamate responsiveness enhanced in neurones expressing amyloid precursor protein. *Neuroreport.* 1997;8:2067–2072.

32. Naskar R, Vorwerk CK, Dreyer EB. Concurrent downregulation of a glutamate transporter and receptor in glaucoma. *Invest Ophthalmol Vis Sci.* 2000;41:1940–1944.

33. Morrison JC, Moore CG, Deppmeier LM, Gold BG, Meshul CK, Johnson EC. A rat model of chronic pressure-induced optic nerve damage. *Exp Eye Res.* 1997;64:85–96.

34. WoldeMussie E, Ruiz G, Feldmann B. Effect of chronically elevated intraocular pressure on loss of retinal ganglion cells in rats [ARVO Abstract]. *Invest Ophthalmol Vis Sci.* 1997;38(4):S159. Abstract nr 787.

35. McKinnon SJ, Pease ME, WoldeMussie E, et al. Comparison of three models of rat glaucoma caused by chronic intraocular pressure elevation [ARVO Abstract]. *Invest Ophthalmol Vis Sci.* 1999;40:S787. Abstract nr 4145.

36. Sanchez RM, Dunkelberger GR, Quigley HA. The number and diameter distribution of axons in the monkey optic nerve. *Invest Ophthalmol Vis Sci.* 1986;27:1342–1350.

37. Lutty GA, Merges C, Threlkeld AB, Crone S, McLeod DS. Heterogeneity in localization of isoforms of TGF-beta in human retina, vitreous, and choroid. *Invest Ophthalmol Vis Sci.* 1993;34:477–487.

38. Lutty G, Ikeda K, Chandler C, McLeod DS. Immunohistochemical localization of transforming growth factor-beta in human photoreceptors. *Curr Eye Res.* 1991;10:61–74.

39. Berkelaar M, Clarke DB, Wang YC, Bray GM, Aguayo AJ. Axotomy results in delayed death and apoptosis of retinal ganglion cells in adult rats. *J Neurosci.* 1994;14:4368–4374.

40. Levin LA, Schlamp CL, Spieldoch RL, Geszvain KM, Nickells RW. Identification of the bcl-2 family of genes in the rat retina. *Invest Ophthalmol Vis Sci.* 1997;38:2545–2553.

41. Levin LA, Louhab A. Apoptosis of retinal ganglion cells in anterior ischemic optic neuropathy. *Arch Ophthalmol.* 1996;114:488–491.

42. Minckler DS, Bunt AH, Johanson GW. Orthograde and retrograde axoplasmic transport during acute ocular hypertension in the monkey. *Invest Ophthalmol Vis Sci.* 1977;16:426–441.

43. McKerracher L, Essagian C, Aguayo AJ. Temporal changes in beta-tubulin and neurofilament mRNA levels after transection of adult rat retinal ganglion cell axons in the optic nerve. *J Neurosci.* 1993;13:2617–2626.

44. Johnson EC, Deppmeier LM, Wentzien SK, Hsu I, Morrison JC. Chronology of optic nerve head and retinal responses to elevated intraocular pressure. *Invest Ophthalmol Vis Sci.* 2000;41:431–442.

45. Muzio M, Chinnaiyan AM, Kischkel FC, et al. FLICE, a novel FADD-homologous ICE/CED-3-like protease, is recruited to the CD95 (Fas/APO-1) death-inducing signaling complex. *Cell.* 1996;85:817–827.

46. Tezel G, Wax MB. Inhibition of caspase activity in retinal cell apoptosis induced by various stimuli in vitro. *Invest Ophthalmol Vis Sci.* 1999;40:2660–2667.

47. Tezel G, Li LY, Patil RV, Wax MB. Tnf-alpha and tnf-alpha receptor-1 in the retina of normal and glaucomatous eyes. *Invest Ophthalmol Vis Sci.* 2001;42:1787–1794.

48. Barnes NY, Li L, Yoshikawa K, Schwartz LM, Oppenheim RW, Milligan CE. Increased production of amyloid precursor protein provides a substrate for caspase-3 in dying motoneurons. *J Neurosci.* 1998;18:5869–5880.

49. Borg JP, Yang Y, De Taddeo-Borg M, Margolis B, Turner RS. The X11alpha protein slows cellular amyloid precursor protein processing and reduces Abeta40 and Abeta42 secretion. *J Biol Chem.* 1998;273:14761–14766.

50. Zambrano N, Minopoli G, de Candia P, Russo T. The Fe65 adaptor protein interacts through its PID1 domain with the transcription factor CP2/LSF/LBP1. *J Biol Chem.* 1998;273:20128–20133.

51. Uetsuki T, Takemoto K, Nishimura I, et al. Activation of neuronal caspase-3 by intracellular accumulation of wild- type Alzheimer amyloid precursor protein. *J Neurosci.* 1999;19:6955–6964.

52. Weidemann A, Paliga K, Dürrwang U, et al. Proteolytic processing of the Alzheimer's disease amyloid precursor protein within its cytoplasmic domain by caspase-like proteases. *J Biol Chem*. 1999;274:5823–5829.

53. Anderson DR, Hendrickson A. Effect of intraocular pressure on rapid axoplasmic transport in monkey optic nerve. *Invest Ophthalmol*. 1974;13:771–783.

54. Quigley HA, Addicks EM, Green WR, Maumenee AE. Optic nerve damage in human glaucoma. II: the site of injury and susceptibility to damage. *Arch Ophthalmol*. 1981;99:635–649.

55. Nishimura I, Uetsuki T, Dani SU, et al. Degeneration in vivo of rat hippocampal neurons by wild-type Alzheimer amyloid precursor protein overexpressed by adenovirus-mediated gene transfer. *J Neurosci*. 1998;18:2387–2398.

56. Kang J, Lemaire HG, Unterbeck A, et al. The precursor of Alzheimer's disease amyloid A4 protein resembles a cell-surface receptor. *Nature*. 1987;325:733–736.

57. Ivins KJ, Thornton PL, Rohn TT, Cotman CW. Neuronal apoptosis induced by beta-amyloid is mediated by caspase-8. *Neurobiol Dis*. 1999;6:440–449.

58. Marin N, Romero B, Bosch-Morell F, et al. beta-amyloid-induced activation of caspase-3 in primary cultures of rat neurons. *Mech Ageing Dev*. 2000;119:63–67.

59. Nakagawa T, Zhu H, Morishima N, et al. Caspase-12 mediates endoplasmic-reticulum-specific apoptosis and cytotoxicity by amyloid-beta. *Nature*. 2000;403:98–103.

60. Tamaoka A, Kalaria RN, Lieberburg I, Selkoe DJ. Identification of a stable fragment of the Alzheimer amyloid precursor containing the beta-protein in brain microvessels. *Proc Natl Acad Sci USA*. 1992;89:1345–1349.

61. Russo C, Salis S, Dolcini V, et al. Identification of amino-terminally and phosphotyrosine-modified carboxy-terminal fragments of the amyloid precursor protein in Alzheimer's disease and Down's syndrome brain. *Neurobiol Dis*. 2001;8:173–180.

62. Rohn TT, Head E, Su JH, et al. Correlation between caspase activation and neurofibrillary tangle formation in Alzheimer's disease. *Am J Pathol*. 2001;158:189–198.

63. Vickers JC, Lazzarini RA, Riederer BM, Morrison JH. Intraperikaryal neurofilamentous accumulations in a subset of retinal ganglion cells in aged mice that express a human neurofilament gene. *Exp Neurol*. 1995;136:266–269.

64. Vickers JC. The cellular mechanism underlying neuronal degeneration in glaucoma: parallels with Alzheimer's disease. *Aust N Z J Ophthalmol*. 1997;25:105–109.

65. Kerrigan-Baumrind LA, Quigley HA, Pease ME, Kerrigan DF, Mitchell RS. Number of ganglion cells in glaucoma eyes compared with threshold visual field tests in the same persons. *Invest Ophthalmol Vis Sci*. 2000;41:741–748.

66. Katzman R. Alzheimer's disease. *N Engl J Med*. 1986;314:964–973.

67. Masliah E, Mallory M, Alford M, Tanaka S, Hansen LA. Caspase dependent DNA fragmentation might be associated with excitotoxicity in Alzheimer disease. *J Neuropathol Exp Neurol*. 1998;57:1041–1052.

68. Yucel YH, Zhang Q, Gupta N, Kaufman PL, Weinreb RN. Loss of neurons in magnocellular and parvocellular layers of the lateral geniculate nucleus in glaucoma. *Arch Ophthalmol*. 2000;118:378–384.

69. Dreyer EB, Pan ZH, Storm S, Lipton SA. Greater sensitivity of larger retinal ganglion cells to NMDA-mediated cell death. *Neuroreport*. 1994;5:629–631.

70. Ishii K, Muelhauser F, Liebl U, et al. Subacute NO generation induced by Alzheimer's beta-amyloid in the living brain: reversal by inhibition of the inducible NO synthase. *FASEB J*. 2000;14:1485–1489.

71. Blanks JC, Hinton DR, Sadun AA, Miller CA. Retinal ganglion cell degeneration in Alzheimer's disease. *Brain Res*. 1989;501:364–372.

72. Sadun AA, Bassi CJ. Optic nerve damage in Alzheimer's disease. *Ophthalmology*. 1990;97:9–17.

73. Tsai CS, Ritch R, Schwartz B, et al. Optic nerve head and nerve fiber layer in Alzheimer's disease. *Arch Ophthalmol*. 1991;109:199–204.

74. LaFerla FM, Tinkle BT, Bieberich CJ, Haudenschild CC, Jay G. The Alzheimer's A beta peptide induces neurodegeneration and apoptotic cell death in transgenic mice. *Nat Genet*. 1995;9:21–30.

75. Blanks JC, Torigoe Y, Hinton DR, Blanks RH. Retinal pathology in Alzheimer's disease. I: ganglion cell loss in foveal/parafoveal retina. *Neurobiol Aging*. 1996;17:377–384.

76. Curcio CA, Drucker DN. Retinal ganglion cells in Alzheimer's disease and aging. *Ann Neurol*. 1993;33:248–257.

77. Citron M, Oltersdorf T, Haass C, et al. Mutation of the beta-amyloid precursor protein in familial Alzheimer's disease increases beta-protein production. *Nature*. 1992;360:672–674.

78. Holcomb L, Gordon MN, McGowan E, et al. Accelerated Alzheimer-type phenotype in transgenic mice carrying both mutant amyloid precursor protein and presenilin 1 transgenes. *Nat Med*. 1998;4:97–100.

79. LeBlanc A. Increased production of 4 kDa amyloid beta peptide in serum deprived human primary neuron cultures: possible involvement of apoptosis. *J Neurosci*. 1995;15:7837–7846.

80. Smale G, Nichols NR, Brady DR, Finch CE, Horton WE Jr. Evidence for apoptotic cell death in Alzheimer's disease. *Exp Neurol*. 1995;133:225–230.

81. Mattson MP. Cellular actions of beta-amyloid precursor protein and its soluble and fibrillogenic derivatives. *Physiol Rev*. 1997;77:1081–1132.

82. Tong L, Thornton PL, Balazs R, Cotman CW. beta-Amyloid-(1–42) impairs activity-dependent cAMP-response element binding protein signaling in neurons at concentrations in which cell survival is not compromised. *J Biol Chem*. 2001;276:17301–17306.

83. Li QX, Maynard C, Cappai R, et al. Intracellular accumulation of detergent-soluble amyloidogenic A beta fragment of Alzheimer's disease precursor protein in the hippocampus of aged transgenic mice. *J Neurochem*. 1999;72:2479–2487.

84. Klein WL, Krafft GA, Finch CE. Targeting small Abeta oligomers: the solution to an Alzheimer's disease conundrum? *Trends Neurosci*. 2001;24:219–224.

85. Raina AK, Hochman A, Zhu X, et al. Abortive apoptosis in Alzheimer's disease. *Acta Neuropathol (Berl)*. 2001;101:305–310.

86. Weisenberg RC, Flynn J, Gao BC, et al. Microtubule gelation-contraction: essential components and relation to slow axonal transport. *Science*. 1987;238:1119–1122.

87. Janicke RU, Ng P, Sprengart ML, Porter AG. Caspase-3 is required for alpha-fodrin cleavage but dispensable for cleavage of other death substrates in apoptosis. *J Biol Chem*. 1998;273:15540–15545.

88. Su JH, Satou T, Anderson AJ, Cotman CW. Up-regulation of Bcl-2 is associated with neuronal DNA damage in Alzheimer's disease. *Neuroreport*. 1996;7:437–440.

89. Holcik M, Gibson H, Korneluk RG. XIAP: apoptotic brake and promising therapeutic target. *Apoptosis*. 2001;6:253–261.

90. Nagy ZS, Esiri MM. Apoptosis-related protein expression in the hippocampus in Alzheimer's disease. *Neurobiol Aging*. 1997;18:565–571.

91. Troy CM, Rabacchi SA, Hohl JB, Angelastro JM, Greene LA, Shelanski ML. Death in the balance: alternative participation of the caspase-2 and -9 pathways in neuronal death induced by nerve growth factor deprivation. *J Neurosci*. 2001;21:5007–5016.

92. Zhang Y, Goodyer C, LeBlanc A. Selective and protracted apoptosis in human primary neurons microinjected with active caspase-3, -6, -7, and -8. *J Neurosci*. 2000;20:8384–8389.

93. Neufeld AH, Sawada A, Becker B. Inhibition of nitric-oxide synthase 2 by aminoguanidine provides neuroprotection of retinal ganglion cells in a rat model of chronic glaucoma. *Proc Natl Acad Sci USA*. 1999;96:9944–9948.

94. Chaudhary P, Ahmed F, Sharma SC. MK801: a neuroprotectant in rat hypertensive eyes. *Brain Res*. 1998;792:154–158.

95. Ko ML, Hu DN, Ritch R, Sharma SC. The combined effect of brain-derived neurotrophic factor and a free radical scavenger in experimental glaucoma. *Invest Ophthalmol Vis Sci*. 2000;41:2967–2971.

96. Kermer P, Klocker N, Labes M, Bahr M. Inhibition of CPP32-like proteases rescues axotomized retinal ganglion cells from secondary cell death in vivo. *J Neurosci*. 1998;18:4656–4662.

97. Kugler S, Klocker N, Kermer P, Isenmann S, Bahr M. Transduction of axotomized retinal ganglion cells by adenoviral vector administration at the optic nerve stump: an in vivo model system for the inhibition of neuronal apoptotic cell death. *Gene Ther*. 1999;6:1759–1767.